On Pilot Design for Wideband Sparse MIMO Channels

Phil Schniter

February 23, 2016

1 Channel Model

Consider the wideband MIMO channel characterized by impulse response $\{\boldsymbol{H}[l]\}_{l=0}^{L-1}$, where $\boldsymbol{H} \in \mathbb{C}^{N_\mathrm{r} \times N_\mathrm{t}}$ and where $N_\mathrm{t}, N_\mathrm{r}, L$ denote the number of transmit antennas, receive antennas, and taps, respectively. If $\boldsymbol{t}[n] \in \mathbb{C}^{N_\mathrm{t}}$ is transmitted over the channel, then the receiver sees $\boldsymbol{y}[n] = \boldsymbol{z}[n] + \boldsymbol{w}[n]$ with

$$\boldsymbol{z}[n] = \sum_{l=0}^{L-1} \boldsymbol{H}[l]\boldsymbol{t}[n-l] \tag{1}$$

and AWGN $\boldsymbol{w}[n]$. Likewise, if the N-symbol sequence $\boldsymbol{T} \in \mathbb{C}^{N_\mathrm{t} \times N}$ is transmitted, the receiver sees $\boldsymbol{Y} = \boldsymbol{Z} + \boldsymbol{W}$ with

$$\boldsymbol{Z} = \begin{bmatrix} \boldsymbol{H}[0] & \boldsymbol{H}[1] & \cdots & \boldsymbol{H}[L-1] \end{bmatrix} \begin{bmatrix} \boldsymbol{T}\boldsymbol{J}_0 \\ \boldsymbol{T}\boldsymbol{J}_1 \\ \vdots \\ \boldsymbol{T}\boldsymbol{J}_{L-1} \end{bmatrix} \tag{2}$$

and AWGN $\boldsymbol{W}$, where right multiplication by $\boldsymbol{J}_l$ circularly shifts the columns right by l places.

Let us now define the virtual channel coefficients

$$\boldsymbol{X}[l] \triangleq \boldsymbol{B}_{N_\mathrm{r}}^* \boldsymbol{H}[l] \boldsymbol{B}_{N_\mathrm{t}}, \tag{3}$$

where

$$\boldsymbol{B}_N \triangleq \boldsymbol{F}_{\sqrt{N}} \otimes \boldsymbol{F}_{\sqrt{N}}, \tag{4}$$

is the steering vector matrix for an N-antenna uniform square array and $\boldsymbol{F}_N$ is the unitary N-DFT matrix. Note that $\boldsymbol{B}_N$ is symmetric and unitary, so that

$$\boldsymbol{H}[l] \triangleq \boldsymbol{B}_{N_\mathrm{r}} \boldsymbol{X}[l] \boldsymbol{B}_{N_\mathrm{t}}^*, \tag{5}$$

The virtual channel coefficients $\{\boldsymbol{X}[l]\}$ are expected to be sparse, which can be exploited in channel estimation. Thus, we rewrite (2) in terms of $\{\boldsymbol{X}[l]\}$ as

$$\boldsymbol{Z} = \boldsymbol{B}_{N_\mathrm{r}} \underbrace{\begin{bmatrix} \boldsymbol{X}[0] & \boldsymbol{X}[1] & \cdots & \boldsymbol{X}[L-1] \end{bmatrix}}_{\triangleq \boldsymbol{X}} \underbrace{\begin{bmatrix} \boldsymbol{B}_{N_\mathrm{t}}^* & & & \\ & \boldsymbol{B}_{N_\mathrm{t}}^* & & \\ & & \ddots & \\ & & & \boldsymbol{B}_{N_\mathrm{t}}^* \end{bmatrix}}_{= \boldsymbol{I}_L \otimes \boldsymbol{B}_{N_\mathrm{t}}^*} \underbrace{\begin{bmatrix} \boldsymbol{T}\boldsymbol{J}_0 \\ \boldsymbol{T}\boldsymbol{J}_1 \\ \vdots \\ \boldsymbol{T}\boldsymbol{J}_{L-1} \end{bmatrix}}_{\triangleq \widetilde{\boldsymbol{T}}}. \tag{6}$$

2 Pilot Design

We are interested in a pilot sequence $\boldsymbol{T}$ for which:

1. there is a fast way of computing $\boldsymbol{Z}$ from a given $\boldsymbol{X}$,
2. $\widetilde{\boldsymbol{T}}$ has a flat singular-value spectrum,
3. $\widetilde{\boldsymbol{T}}$ has low peak-to-average power ratio (PAPR).

Towards this aim, we propose to construct $\boldsymbol{T}$ such that

$$[\boldsymbol{T}]_{n,m} = t[\langle nL + m\rangle_N], \tag{7}$$

where $N, \sqrt{N_\mathrm{t}}, \sqrt{N_\mathrm{r}}$ are all powers of two, $N \geq N_\mathrm{t}L$, and $\{t[n]\}_{n=0}^{N-1}$ has good low PAPR and thumbtack-like periodic-autocorrelation over $N_\mathrm{t}L$ lags, e.g.,

a) random BPSK,

b) chirp/Chu sequence, i.e., $t[n] = \exp(j\pi n^2/N)$ for $n = 0...N-1$.

Note that both of the above are constant modulus, and thus they have optimal PAPR. The chirp/Chu sequence has also has perfect periodic-autocorrelation over N lags, where by construction $N \geq N_\mathrm{t}L$.

The reasoning behind (7) is that the rows of $\widetilde{\boldsymbol{T}}$ will consist of the first $N_\mathrm{t}L$ circular shifts of the sequence $\boldsymbol{t} \triangleq \big[t[0] \ \ldots \ t[N-1]\big]$, and thus multiplication by $\widetilde{\boldsymbol{T}}$ can be accomplished using fast convolution with N-FFTs. Note that the operations involving $\boldsymbol{B}_{N_\mathrm{t}}$ and $\boldsymbol{B}_{N_\mathrm{r}}$ can also be accomplished using $\sqrt{N_\mathrm{t}}$-FFTs and $\sqrt{N_\mathrm{r}}$-FFTs, respectively.

Figure 1 plots the singular values for one realization of $\widetilde{\boldsymbol{T}}$ under the two choices of $\boldsymbol{t}$ above. For reference, it also shows the singular values for one realization of $\widetilde{\boldsymbol{T}}$ with i.i.d. Gaussian entries (i.e., no convolution structure), which is the form of the matrix assumed in the derivation of GAMP. The figure shows that the convolution matrix $\widetilde{\boldsymbol{T}}$ constructed using random BPSK $\boldsymbol{t}$ has a similar spectrum to the i.i.d. Gaussian $\widetilde{\boldsymbol{T}}$. It also shows that the chirp/Chu sequence has a flat singular value spectrum, which may or lead to improved GAMP performance (need to check).

3 Fast Implementation

We now provide some details on the fast implementation of (6). Recall that, due to the construction (7), the first N_t rows in $\widetilde{\boldsymbol{T}}$ contain the $\{0, L, 2L, ..., (N_\mathrm{t}-1)L\}$ shifts of $\boldsymbol{t}$. Likewise, the next N_t rows in $\widetilde{\boldsymbol{T}}$ contain the $\{1, L+1, 2L+1, ..., (N_\mathrm{t}-1)L+1\}$ shifts of $\boldsymbol{t}$, and the last N_t rows in $\widetilde{\boldsymbol{T}}$ contain the $\{L-1, 2L-1, 3L-1, ..., N_\mathrm{t}L-1\}$ shifts of $\boldsymbol{t}$. Altogether, the rows of $\widetilde{\boldsymbol{T}} \in \mathbb{C}^{N_\mathrm{t}L\times N}$ contain the $\{0, 1, 2, \ldots, N_\mathrm{t}L\}$ shifts of $\boldsymbol{t}$. We can thus re-order the rows in $\widetilde{\boldsymbol{T}}$ to make $\widetilde{\boldsymbol{T}}$ a Toeplitz matrix, which we will denote by $\overline{\boldsymbol{T}}$ in the sequel. Doing so yields

$$\begin{aligned}
\boldsymbol{Z} &= \boldsymbol{B}_{N_\mathrm{r}}\boldsymbol{X}\left[\begin{array}{cccc|cccc|c|cccc}
\boldsymbol{b}_0 & & & & \boldsymbol{b}_1 & & & & \cdots & \boldsymbol{b}_{N_\mathrm{t}-1} & & & \\
& \boldsymbol{b}_0 & & & & \boldsymbol{b}_1 & & & \cdots & & \boldsymbol{b}_{N_\mathrm{t}-1} & & \\
& & \ddots & & & & \ddots & & \cdots & & & \ddots & \\
& & & \boldsymbol{b}_0 & & & & \boldsymbol{b}_1 & \cdots & & & & \boldsymbol{b}_{N_\mathrm{t}-1}
\end{array}\right]\overline{\boldsymbol{T}} && (8)\\
&= \boldsymbol{B}_{N_\mathrm{r}}\underbrace{\big[\,\boldsymbol{x}_0[0]\cdots\boldsymbol{x}_0[L-1]\,\big|\,\boldsymbol{x}_1[0]\cdots\boldsymbol{x}_1[L-1]\,\big|\cdots\boldsymbol{x}_{N_\mathrm{t}-1}[0]\,\big|\cdots\boldsymbol{x}_{N_\mathrm{t}-1}[L-1]\big]}_{\triangleq\,\overline{\boldsymbol{X}}^\mathsf{T}}\big(\boldsymbol{B}_{N_\mathrm{t}}^*\otimes\boldsymbol{I}_L\big)\overline{\boldsymbol{T}} && (9)\\
&= \boldsymbol{B}_{N_\mathrm{r}}\Big[\overline{\boldsymbol{T}}^\mathsf{T}\big(\boldsymbol{B}_{N_\mathrm{t}}^*\otimes\boldsymbol{I}_L\big)\overline{\boldsymbol{X}}\Big]^\mathsf{T}, && (10)
\end{aligned}$$

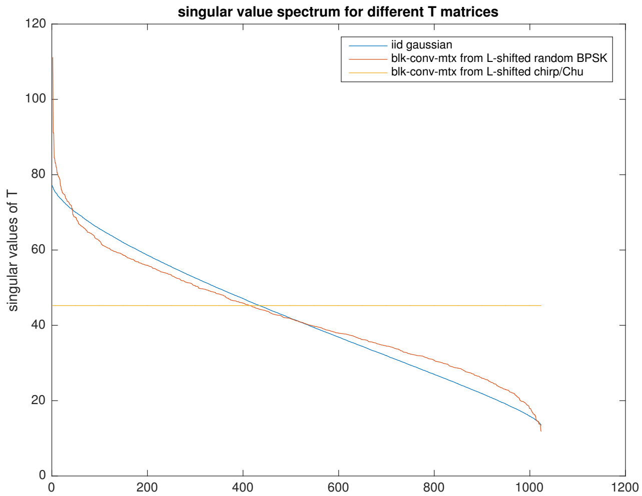

Figure 1: Singular values of $\widetilde{\boldsymbol{T}}$ for various constructions of $\boldsymbol{t}$.

where $\boldsymbol{b}_i$ is the ith column of $\boldsymbol{B}_{N_\mathrm{t}}*$ and $\boldsymbol{x}_i[l]$ is the ith column of $\boldsymbol{X}[l]$. For the last equality above, we exploited the fact $(\boldsymbol{A} \otimes \boldsymbol{B})^\mathsf{T} = \boldsymbol{A}^\mathsf{T} \otimes \boldsymbol{B}^\mathsf{T}$ and the symmetry of $\boldsymbol{B}^*_{N_\mathrm{t}}$.

The fast implementation of (10) is now visible. First, for any $\boldsymbol{v} \in \mathbb{C}^{LN_\mathrm{t}}$, notice that

$$\big(\boldsymbol{B}^*_{N_\mathrm{t}} \otimes \boldsymbol{I}_L\big)\boldsymbol{v} = \mathrm{vec}(\boldsymbol{V}\boldsymbol{B}^*_{N_\mathrm{t}}) = \mathrm{vec}([\boldsymbol{B}_{N_\mathrm{t}}\boldsymbol{V}^\mathsf{H}]^\mathsf{H}), \tag{11}$$

where $\boldsymbol{V} \in \mathbb{C}^{L \times N_\mathrm{t}}$ is the column-wise matricization of $\boldsymbol{v}$. Furthermore, for any $\boldsymbol{u} \in \mathbb{C}^{N_\mathrm{t}}$, notice that

$$\boldsymbol{B}_{N_\mathrm{t}}\boldsymbol{u} = \big(\boldsymbol{F}_{\sqrt{N_\mathrm{t}}} \otimes \boldsymbol{F}_{\sqrt{N_\mathrm{t}}}\big)\boldsymbol{u} = \mathrm{vec}(\boldsymbol{F}_{\sqrt{N_\mathrm{t}}}\boldsymbol{U}\boldsymbol{F}_{\sqrt{N_\mathrm{t}}}), \tag{12}$$

where $\boldsymbol{U} \in \mathbb{C}^{\sqrt{N_\mathrm{t}} \times \sqrt{N_\mathrm{t}}}$ is the column-wise matricization of $\boldsymbol{u}$. Thus the multiplication $\big(\boldsymbol{B}^*_{N_\mathrm{t}} \otimes \boldsymbol{I}_L\big)\overline{\boldsymbol{X}}$ in (10) can be accomplished using $\sqrt{N_\mathrm{t}}$-point FFTs. The result of that multiplication is then left-multiplied by $\overline{\boldsymbol{T}}^\mathsf{T}$, which can be performed via fast convolution using N_r FFTs of length N. And the result of that multiplication is then left-multiplied by $\boldsymbol{B}_{N_\mathrm{t}}$, which can be performed as in (12) using $\sqrt{N_\mathrm{t}}$-point FFTs. [Should count how many total FFTs of each length.]

4 Faster Implementation

The complexity of the solution above, which relies on N-point FFTs and $N \geq N_\mathrm{r}L$, is probably still too high, it can be reduced by choosing $\boldsymbol{t} = [1, 0, 0, ..., 0]$, which turns $\overline{\boldsymbol{T}}$ into an $N_\mathrm{t}L \times N$ identity matrix. The cost is a drastic reduction in SNR. Still, it may be worth investigating as an option.